Extension of Summer Climatic Conditions into Spring in the Western Mediterranean Area

Pre-print of:

Jansa A, Homar V, Romero R, Alonso S, Guijarro JA, Ramis C (2016): Extension of summer climatic conditions into spring in the Western Mediterranean area. *Int. J. Climatol.*, 13 pp, DOI: 10.1002/joc.4824.

A. Jansa[1], V. Homar[1], R. Romero[1], S. Alonso[1,2], J.A. Guijarro[3] and C. Ramis[1]

[1] *University of the Balearic Islands (UIB), Physics Dpt., Group de Meteorology, Palma, Mallorca, Spain*

[2] *Institut Mediterrani d'Estudis Avançats (IMEDEA), Global Change Research Dpt., Palma, Mallorca, Spain*

[3] *State Meteorological Agency (AEMET), Balearic Is. Office, Palma, Mallorca, Spain*

Correspondence: agusti.jansa@gmail.com

Key words: Mediterranean, summer, spring, expansion, Hadley cell, deep subtropical anticyclone, climate change

Abstract

From a local point of view, in May/June there is an important and positive 2 m temperature trend at Palma (Mallorca), which is simultaneous and highly correlated with a strong increase in the 500 hPa geopotential height. The present study analyses this fact as well as the observed tendencies in a wider seasonal and geographical context.

We confirm the particularly high correlation between 2 m temperature and 500 hPa geopotential during the warm months as opposed to the much weaker correlation in winter. This suggests that mechanisms for thermal changes act differently throughout the year in this region. Besides the direct radiative effect, warm season near-surface temperatures are linked to the presence of deep anticyclones, which effectively determine the northen edge of the Hadley cell. Accordingly, the strong warming trend in the area of Palma during the warm months of the year is purportedly related to the poleward extension of the Hadley cell.

The fact that May/June show the highest low-level temperature trend among all bimonthly series is a common regional feature over a relatively wide area over the Western Mediterranean. Different geographical patterns emerge in other periods of the year. In July/August, the strongest low-level warming area drifts to the east-northeast, towards Ukraine and Russia. Coincidentally, the 500 hPa geopotential

tendencies show a coherent pattern, with an intense positive trend ridge over the Western Mediterranean area in May/June, and a displacement of this ridge to the north-east in July/August.

We show the connection between 500 hPa geopotential height and near-surface temperature by means of a multiple lineal regression that attributes half of the local temperature tendency in Palma to the intensification of a 500 hPa ridge centred over the Western Mediterranean and surroundings.

1. Introduction

The near-surface (2 m) temperature trend observed for the 1973-2012 period at the Palma airport (Mallorca, LEPA, Fig. 1), located in Western Mediterranean, is considerably stronger than the global average, but more importantly, it shows a prominent maximum in May/June (MJ) when bimonthly periods are considered. Note that the adoption of the alternative bimonthly periods (AM instead of MJ) renders a higher temperature trend for AM than for MJ; however, we use the calendar-based definition since it enables usto distinguish full-season periods (JA for summer and JF for winter), from the transitional periods (MA, MJ, SO and ND). Focusing the analysis on the transition period from spring to summer, the maximum warming in MJ may be interpreted as an early transition from spring to summer, or, equivalently, as a tendency for summery conditions to occur earlier in the year, resulting in a longer effective summer. Since the warming in MJ is stronger than in SO, the temporal extension of the summery conditions is asymmetric. Similarly, but in terms of rainfall, Ziv et al. (2014) found an enlargement of the dry season in Israel that is also asymmetric, with more intense changes in spring than in autumn.

Jansà (2012) identified a significant correlation between MJ 2 m temperature in Palma and 500 hPa geopotential height (thereinafter referred to as 500-GH) in the observed time series. This link is weaker in other periods of the year and especially poor in winter. Note that the dry/warm and moist/temperate seasons that typify the Mediterranean climate are linked to the alternation between tropical (warm) and extra-tropical (temperate) circulations (Trigo et al., 2006). The Mediterranean summer, in particular, is usually defined and characterised by the dominance of deep and warm subtropical anticyclones (Barry and Chorley, 2010), which effectively determine the poleward edge of the Hadley Cells (HC). That is, the edge of the HC penetrates the Mediterranean region during the summer months due to the latitudinal shift of the whole general atmospheric circulation. The Mediterranean summer conditions (warm/hot and dry period) in Palma are unequivocally identified in July and less clearly in August. In any case, when taking bimonthly periods, JA shows more apparent warm/dry conditions than MJ, for the period 1981-2010 (Fig. 2).

For the Balearic Islands, Homar et al. (2010) analysed three-monthly temperature and rainfall trends, concluding that the highest warming and drying tendencies are both found in spring (MAM), followed by summer (JJA). Combining this analysis with the two-monthly analyses performed by Jansà (2012), the expansion of the Mediterranean summery conditions towards late spring can be seen as an observational fact, at least in the Balearic Islands. In turn, the intense MJ warming observed in Palma is ostensibly associated to a strong increase in the 500-GH, also in MJ (Jansà, 2012), which can be attributed to a more frequent presence of the prominent high 500-GH tropical dome that characterises mid-level HC. These changes appear as a regional and specific expression of a more general, planetary manifestation of climate change, namely, the enlargement of the HC, already detected from multiple perspectives and indicators (IPCC, 2013; Birner et al., 2014).

Figure 1: Area of interest and location of Palma, Mallorca.

Section two below reviews some concepts regarding the Mediterranean climate and summer. Section three analyses observed surface temperature trends focusing on the MJ period. Section four looks at the correlation between near-surface temperature and 500-GH in Palma. Section five analyses the regional distribution of the observed 500-GH bi-monthly tendencies. Section six describes the methodology and results of attribution analysis of the local near-surface warming to the secular evolution of 500 hPa spatial patterns. Finally, section seven offers a brief discussion of the results, including some conclusions.

2. Mediterranean Climate. Mediterranean Summer

According to the Köppen's classification of world climates, the Mediterranean climate (labelled *Cs*) is defined as a mid-latitude temperate climate, where the clearest sign of identity is a dry summer season (Köppen, 1900, Köppen and Geiger, 1930, Lionello et al., 2012). A dry Mediterranean climate would be an appropriate expression for regions with BS climate in which summer is dry with respect to the rest of the year. In fact, the boundary between the Köppen's Cs and BS types has not been defined in exactly the same way by different authors. Köppen-Geiger strict definition has been assumed and validated by authors like Peel et al. (2007), but other formulations such as the Köppen-Trewartha climate classification (Trewartha and Horn, 1980), have been preferred by other researchers (de Castro et al., 2007; Belda et al., 2014). Without a rigorous definition, the concept of Mediterranean climate, including a dry summer, is present in other views about the question (Blumler, 2005).

Although the climate in Palma would be classified as *Cs* or *BS*, depending on the specific criterion chosen, it clearly has a temperate climate, with a dry summer relative to other seasons. We thus consider the climate in Palma as *Mediterranean* or *Dry Mediterranean* (see Fig. 2).

Mediterranean summer conditions are attributed to the influence of the HC, whose northern edge enters the region this season (Trigo et al., 2006, Barry and Chorley, 2010). Therefore, studying the long-term evolution of the region's summer conditions (such as initiation and duration) requires investigation of the long-term evolution of the regional influence of the HC, particularly with regard to the location of its northern edge.

The zonal- mean of the Stokes streamfunction provides a clear depiction of the HC (Hartmann, 1994). The closed circulation is very clearly identified when annual averages are considered. In addition, the HC signature on the zonal mean Stokes streamfunction emerges nicely in spring and fall. However, during summer months in the northen hemisphere, the HC signature fades away considerably, instead of simply shifting northwards, due to disruption of strong regional circulations, such as the Indian monsoons (Dimas and Walace, 2003; Cook, 2005). Therefore, with regard

to the onset, duration or expansion of the Mediterranean summer, the zonal mean of the Stokes streamfunction does not provide a robust and reliable proxy, as already stressed Rodwell and Hoskins (1996). In fact, the Mediterranean climate only covers a limited region, that is, the western flanks of the continental masses, and does not extend along a complete latitudinal band around the planet.

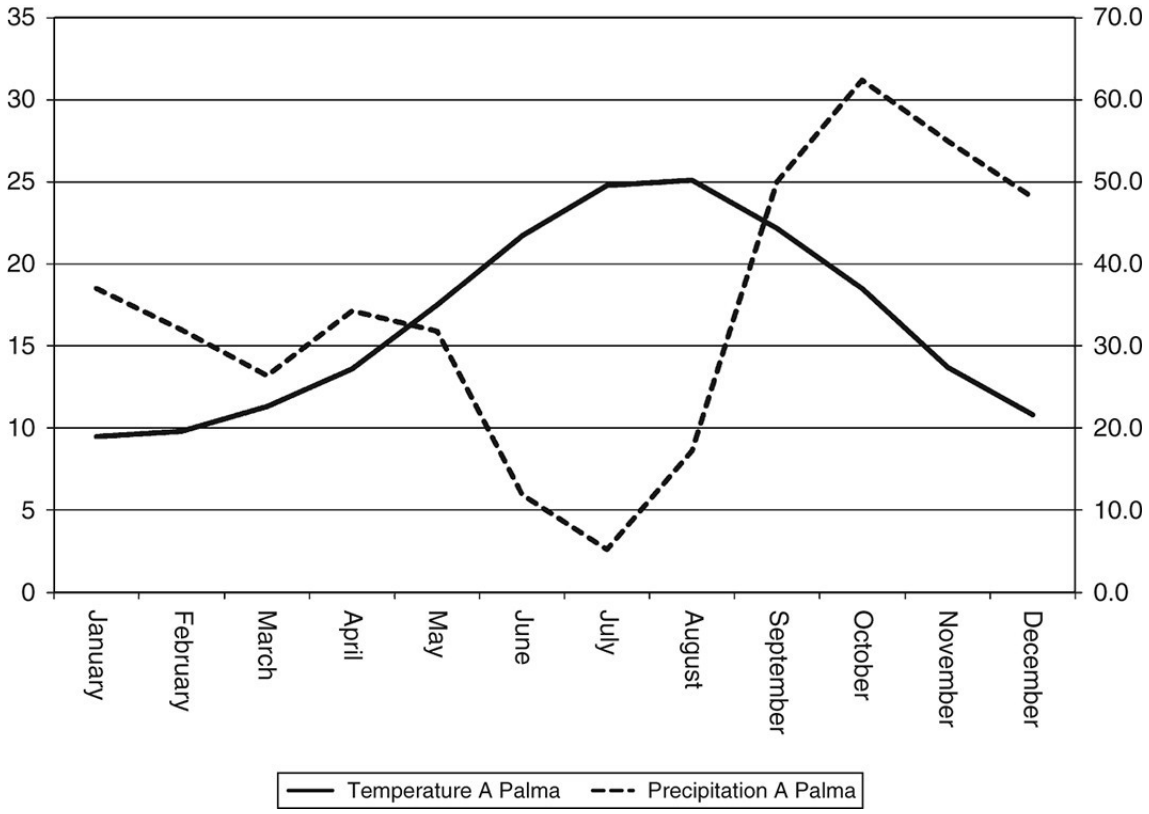

Figure 2: Ombrothermic diagram (monthly distribution of temperature and precipitation; Gaussen, 1955) for Palma airport, 1981–2010. Dry summer is a striking feature. Raw data from AEMET.

In order to identify the northern edge of the summer HC in a limited regional area, including the Mediterranean, we have explored the use of the vertical-meridional mass flux along the 20W-20E segment, as an alternative to the zonal mean Stokes streamfunction. The results (not shown) are significantly distorted, most likely by orographic systems such as the Atlas, Alps and Iberian Peninsula mountain systems, and do not provide a useful depiction of the inter-tropical belt evolution. Similar skewed results emerge when vertical velocity and horizontal divergence fields from the National Center for Environmental Prediction and National Center for Atmospheric Research (NCEP-NCAR) reanalysis (Kalnay et al., 1996) are considered (Fig. 3). The upward branch of the HC is clearly identifiable over a large longitudinal extension around 10°N, however the descending counterpart around 35-40°N is not as manifest. Strong subsidence is observed in the Central and Eastern

Mediterranean, but an ascending nucleus surrounded by weaker subsidence is found in the western part, despite no low-level anticyclonic circulation appearing. Ziv et al. (2004) attributed the subsidence maximum to the combined effect of the Asian Monsoon and HC. In turn, Rodwell and Hoskins (1996) and Hoskins (1996) link this subsidence to a balancing compensation for the Indian Monsoon ascent, produced by means of a westward Rossby wave propagation. These authors associate the upward motion around the southern Iberian Peninsula with warm advection, although some of the structures obtained in Fig. 3 can also result from orographically induced strong convergences and divergences. In fact, strong convergence at low levels (namely, 800 hPa) appears associated with high elevations in North-Africa, suggesting orographic blocking and the subsequent upward motion. Compensatory divergences would appear at high levels, above the region. In addition, divergence at high levels (which promote upwards motion underneath) can also be forced by positive vorticity advection, associated with a weak upper level trough located just westward of the Iberian Peninsula and North Africa, which is visible in the average summer maps (not shown).

Therefore, the attempt to link the Mediterranean summer to the seasonal shifting of the HC seems to lead to confusion in light of its questionable existence (also stressed by Rodwell and Hoskins, 1996). To solve this apparent inconsistency we need to question the significance level of the global zonal mean when strong regional circulations, such as the Indian monsoons, disrupt the zonal homogeneity of the HC circulation. In fact, the Mediterranean climate or dry summer climate only covers a limited region, that is, the western flanks of the continental masses, and is not a complete latitudinal band around the planet: there is no zonal continuum of the Mediterranean climate.

Apart from the Stokes streamfunction, other measures and proxies have been used by different authors to locate the edges of the HC, and therefore to investigate its hypothesised expansion over the last decades. The latitudinal maximum of the outgoing long wave radiation or the latitudinal minimum of the average total precipitation are some examples (Hu and Fu, 2007, Lu et al., 2007, Seidel and Randel, 2007, Fu and Lin, 2011, Kang and Lu, 2012, IPCC, 2013, Birner et al., 2014).

Other indicators rely on the idea that the poleward edge of the HC is a fairly continuous band of subtropical, deep and warm anticyclones. Indeed, several authors have used the latitudinal maximum of sea level pressure (SLP), although results have been neither very clear, nor very consistent (Hu et al., 2011, Li et al., 2012). This is arguably due to the masking effect of the low level temperatures onto SLP. The Mediterranean (dry) anticyclonic summer weather and (wet) cyclonically disturbed winter (Trigo et al., 2006, or Barry and Chorley, 2010, or Guijarro et al., 2006) is not reflected on the SLP observation in Palma (Fig. 4). The annual SLP maximum occurs in winter, particularly in January, when the Western Mediterranean cyclonic activity is strongest. Note that summer SLPs, when cyclonic activity is at its

lowest, are significantly lower than winter values. Monthly SLPs reach their minimum in spring, particularly in April, when intermediate low-level temperatures coincide with frequent cyclonic activity (Guijarro et al., 2006). The effect of low-level temperatures weakens with height, but 850 hPa geopotential values are still impacted (Fig. 4). The monthly averaged for 500-GH, on the contrary, shows a very well defined annual wave, with a maximum in July and August, well above the 5800 gpm level, and a minimum in February and January, below 5630 gpm (Fig. 4). Therefore, 500-GH becomes a robust candidate to investigate the evolution of the onset and duration of summer over the Western Mediterranean, as opposed to the less dynamically relevant SLP field.

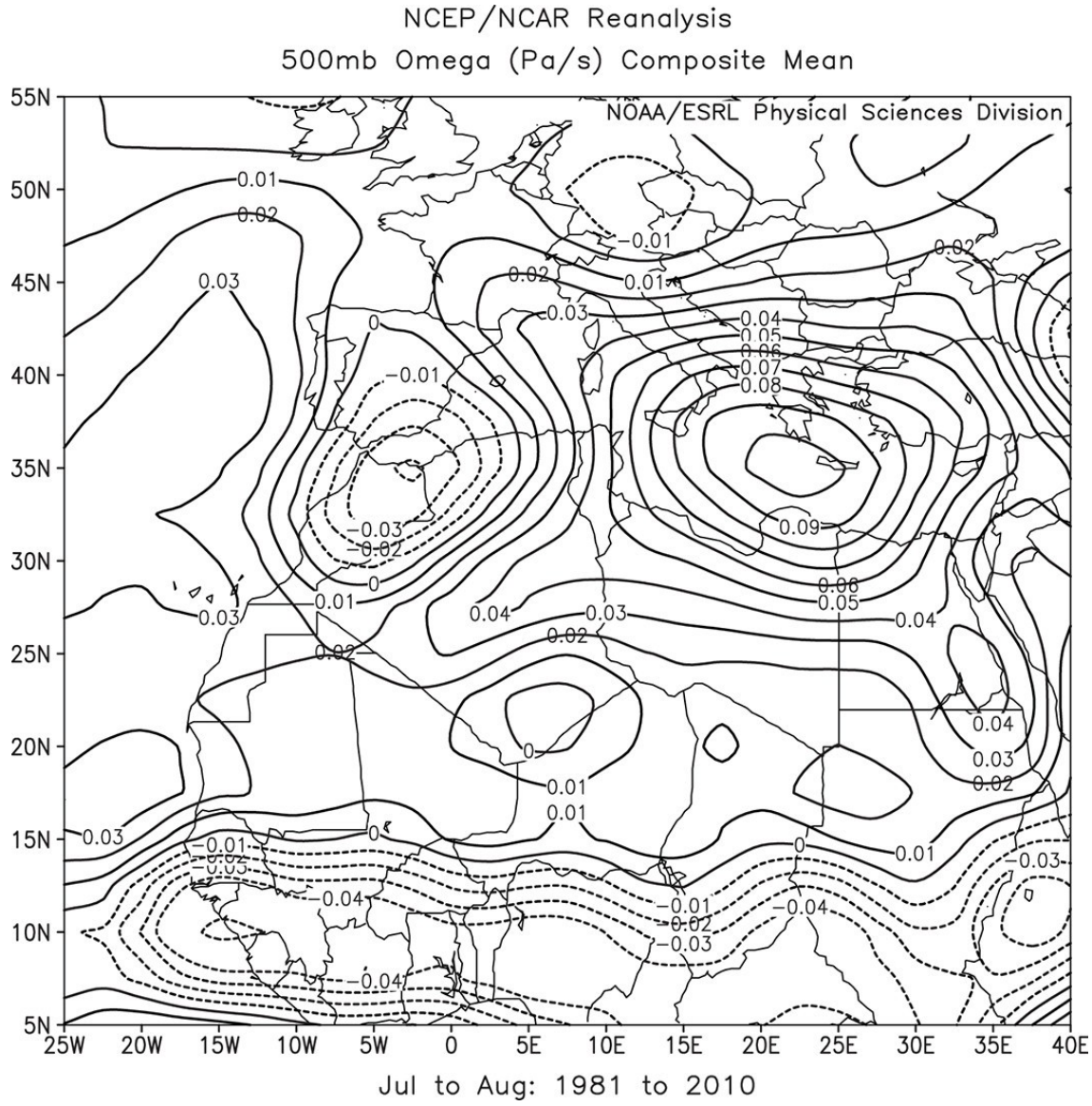

Figure 3 | A 1981–2010 average vertical motion at 500 hPa, during July and August (ω: isolines for every 0.01 Pa s−1; negative (upwards) values are drawn with dashed lines).

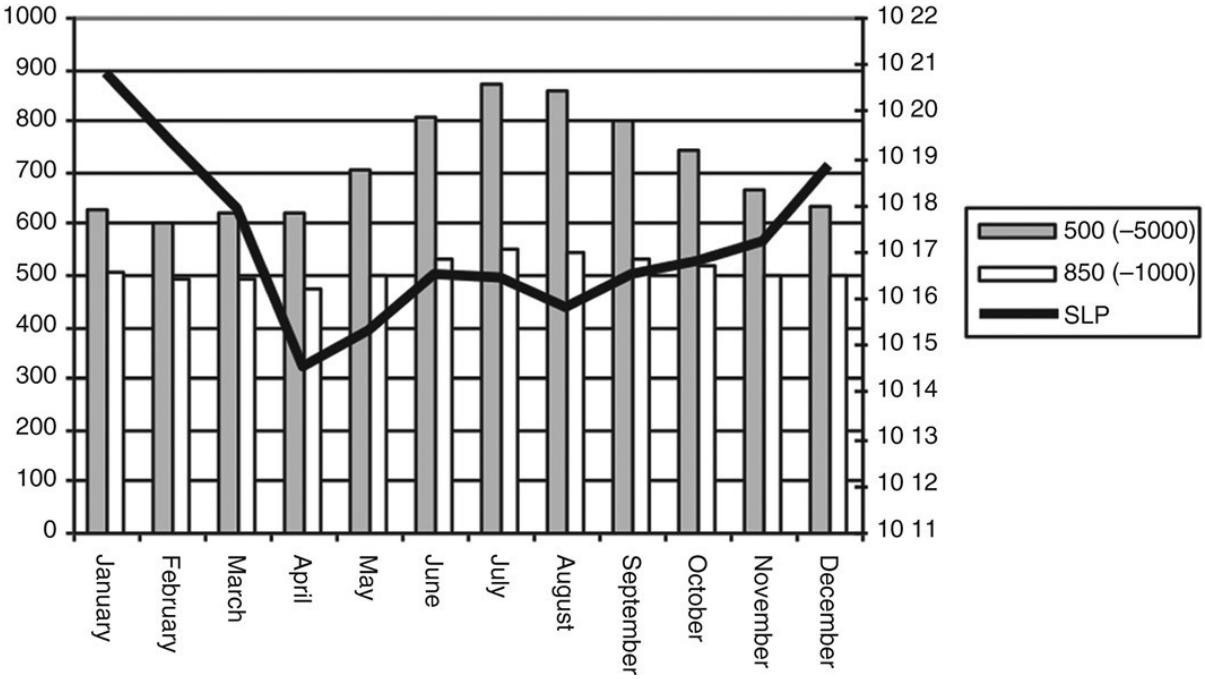

Figure 4: Monthly evolution of SLP and 850 and 500-GH at Palma, Mallorca, 1981–2010.

3. Low-level Observed Temperature Tendencies in Palma and in The Mediterranean Zone

The thermometric station at Palma-airport has been continuously recording daily measurements since 1973, with no change of location being sited far from terminal buildings. In an attempt to remove non-climatic changes in the series, we applied an homogenization procedure by means of the R package *Climatol v. 2.2* (Guijarro, 2014), which uses the SNHT test to detect sudden shifts or local trends to split the series into homogeneous sub-periods in an iterative process, reconstructing all sub-series when there are missing data. After this homogenization step, we perform a least-squares linear regression on the 1973-2012 series and obtained a tendency for the annual mean temperature of 0.43ºC per decade, with trends ranging from 0.78 to 0.70 for the monthly series of April, May and June. These are remarkably high values compared to global mean values (see IPPC, 2013).

The distribution of bi-monthly tendencies throughout the year shows a clear distinction between a single maximum in MJ exceeding 0.7ºC/decade and no significant trends in JF (Fig. 5 and Table 1).

Previous studies are generally consistent with the trends obtained here for Palma. Besides Homar et al. (2010), restricted to the Balearics, de Río et al. (2006) used hundreds of near-surface stations in mainland Spain to derive seasonal trends for 1961-2006, characterised by high positive values in summer and spring and lower values in winter and autumn, with a maximum average of 0.5ºC/decade in June,

including values of 0.7 and 0.8ºC/decade for particular stations or zones. Bladé and Castro-Díez (2010) obtained seasonal trends (1973-2005) of 0.27 and 0.29ºC/decade for winter and autumn, respectively, and 0.77 and 0.67ºC/decade in spring and summer.

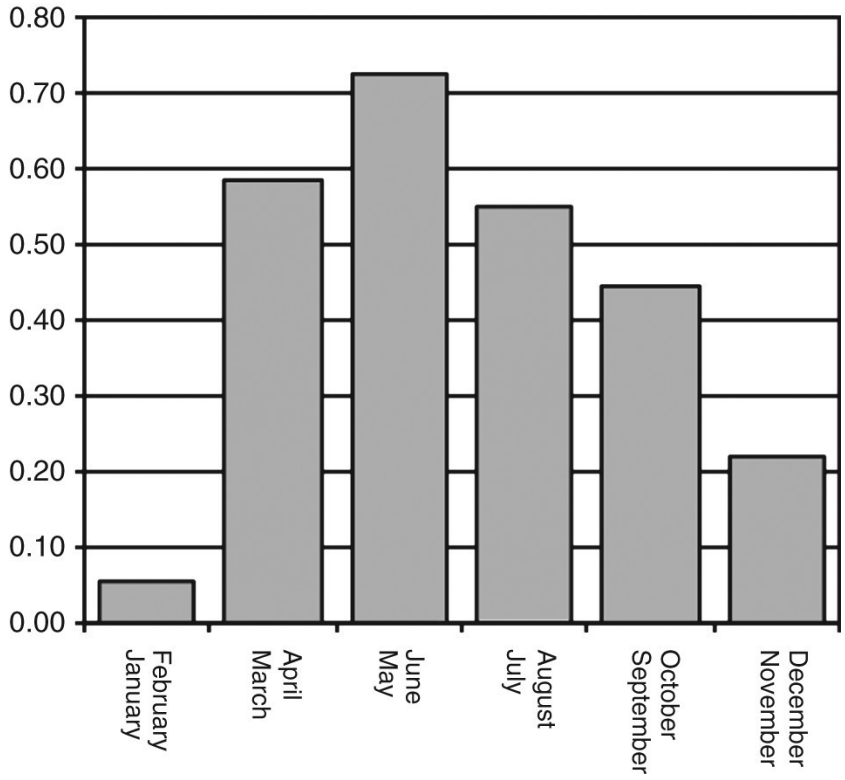

Figure 5 | Bi-monthly temperature tendencies (°C 10 years−1). Palma airport, 1973–2012 homogenized series.

With regard to the whole Mediterranean area, Lionello et al. (2012) inferred higher warming in the Western Mediterranean rather than in the East. Over the Western area, where the largest trends seem to be occurring in areas of Spain, France and Maghreb, summer shows the maximum warming, with 0.4-0.5ºC/decade, followed by spring, fall and winter.

Although spring and early summer monthly trends in some surrounding regions are as high as the local tendencies observed in Palma, seasonal values are significantly smoothed compared to the monthly or even bi-monthly values. The use of different periods to compute temperature tendencies also explain some discrepancies. Even the use and type of homogenisation procedure may alter the resulting trend values.

In order to confirm the regional coherence of the fact that late spring and early summer is the period with the highest trends, Spanish AEMET climatological stations with long raw series have been analysed, using a spatial clustering technique based on hydrological basins and natural regions, as in Guijarro (2013), and using the

1973-2012 period (Table 1 and in Fig. 6). Alternative clustering criteria, based on the homogeneity of thermal values or trends have been used in other studies (e. g. Argüeso et al., 2012).

Regional tendencies for the Balearic Islands (CB) are similar to those obtained for Palma airport, with a slight general reduction, probably attributable to the effect of stations located in Menorca, Ibiza/Eivissa and Formentera, with higher maritime influence. Regarding other Spanish regions, the differentiated behaviour of the Canary Islands region (CC) (with clearly lower tendencies) is another remarkable aspect, but its subtropical location is determinant (Fig. 1).

Table 1. Monthly and bi-monthly 1973-2012 temperature tendencies (ºC/10yrs), local at Palma airport (Pal) and averaged in Spanish main hydrological basins (Cx: see figure 6 for location).

	Pal	CB	C1	C2	C3	C4	C5	C6	C7	C8	C9	C0	CC
Jan	0.11	0.17	0.29	0.20	0.07	-0.02	-0.06	-0.02	0.01	-0.06	-0.12	0.12	0.18
Feb	0.01	0.03	0.16	-0.03	-0.03	0.02	0.06	0.06	-0.02	-0.09	-0.16	-0.03	0.06
Mar	**0.40**	**0.36**	**0.49**	**0.46**	**0.37**	0.38	**0.44**	**0.42**	0.25	0.19	0.17	**0.43**	0.16
Apr	**0.78**	**0.71**	**0.79**	**0.53**	**0.45**	**0.48**	**0.54**	**0.56**	**0.45**	**0.48**	**0.50**	**0.62**	0.18
May	**0.76**	**0.66**	**0.82**	**0.60**	**0.63**	**0.66**	**0.69**	**0.68**	**0.54**	**0.55**	**0.57**	**0.75**	**0.32**
Jun	**0.70**	**0.62**	**0.77**	**0.41**	**0.59**	**0.72**	**0.72**	**0.82**	**0.79**	**0.70**	**0.65**	**0.76**	**0.37**
Jul	**0.56**	**0.43**	**0.44**	0.15	0.18	**0.39**	**0.34**	**0.46**	**0.64**	**0.48**	**0.46**	0.33	0.26
Aug	**0.55**	**0.53**	**0.62**	**0.31**	0.25	**0.42**	**0.39**	**0.47**	**0.57**	**0.53**	**0.53**	**0.47**	0.18
Sep	0.29	0.26	0.25	0.15	0.00	0.10	-0.01	0.01	0.12	0.06	0.07	0.12	-0.13
Oct	**0.60**	**0.63**	**0.69**	**0.41**	0.33	0.38	0.36	**0.42**	**0.41**	**0.40**	**0.41**	**0.52**	0.04
Nov	**0.40**	**0.43**	**0.40**	0.08	0.01	0.01	-0.06	-0.06	-0.01	-0.01	0.00	0.22	-0.09
Dec	0.05	0.11	0.15	-0.05	-0.05	-0.12	-0.10	-0.04	-0.01	-0.10	-0.15	-0.02	0.08
JF	0.06	0.10	0.22	0.08	0.02	0.00	0.00	0.02	-0.01	-0.08	-0.14	0.05	0.12
MA	**0.58**	**0.53**	**0.64**	**0.50**	**0.41**	**0.43**	**0.49**	**0.49**	**0.35**	**0.34**	**0.33**	**0.53**	0.17
MJ	**0.72**	**0.64**	**0.80**	**0.51**	**0.61**	**0.69**	**0.70**	**0.75**	**0.67**	**0.62**	**0.61**	**0.75**	**0.35**
JA	**0.55**	**0.48**	**0.53**	**0.23**	0.22	**0.40**	**0.37**	**0.46**	**0.61**	**0.51**	**0.50**	**0.40**	0.22
SO	**0.45**	**0.44**	**0.47**	**0.28**	0.16	0.24	0.18	0.21	**0.26**	**0.23**	0.24	**0.32**	-0.04
ND	0.22	**0.27**	0.27	0.01	-0.02	-0.05	-0.08	-0.05	-0.01	-0.05	-0.08	0.10	-0.01
Year	**0.43**	**0.41**	**0.49**	**0.27**	**0.23**	**0.28**	**0.28**	**0.31**	**0.31**	**0.26**	**0.24**	**0.36**	**0.13**

*Note: Statistically significant values at a confidence level of 95% or more are represented in **bold** types*

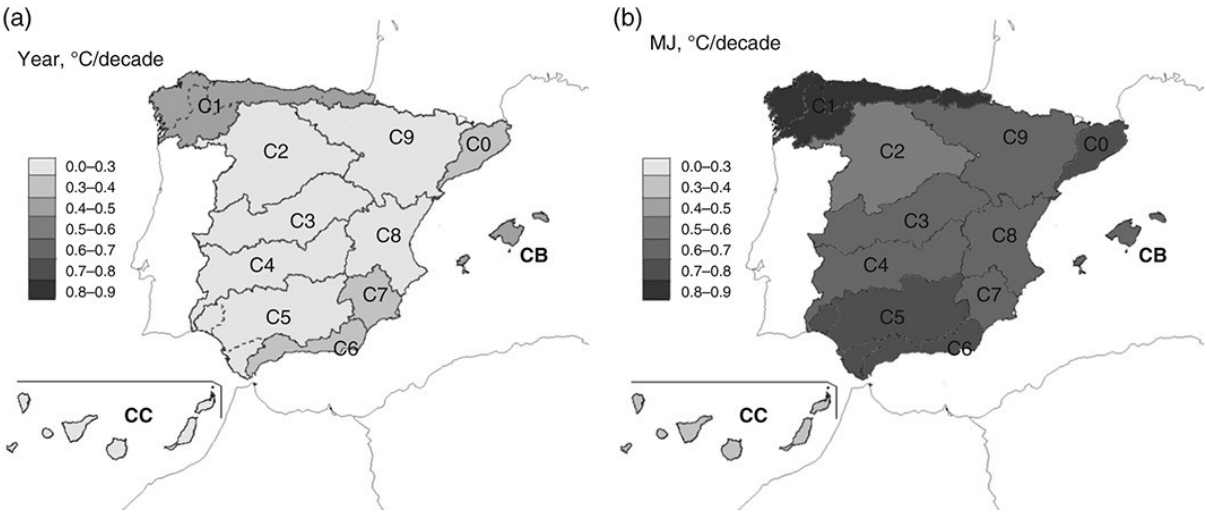

Figure 6: The 2 m temperature tendencies (°C decade−1) of the yearly (a) and bi-monthly MJ (b) homogenized and regionally averaged time series for the period 1973–2012.

There are noticeable differences among the rest of the basins or regions, but common aspects are remarkable. The annual tendencies are above 0.2ºC/decade. Spring and summer tendencies, as well as for October one, are stronger and more statistically robust than values in winter and September. The maximum bi-monthly tendencies appear in MJ throughout Spain.

For the sake of a more spatially comprehensive investigation of the near-surface temperature trends, we use the NCEP_NCAR Reanalysis (Fig. 7). Annual and MJ tendencies over the Iberian Peninsula show a good alignment with the regional results described above, with values around 0.2 and 0.6ºC/decade, respectively. Trends over the Balearics are notably underestimated, most likely due to the inability of the analysis system to reliably simulate the effects of this relatively small archipelago, and resulted in biased maritime analysis fields. The bi-monthly MJ temperatures produce a much stronger warming than the annual average, in the MA and JA series, at least across the Iberian Peninsula, the Western Mediterranean, France and North-west Africa. On the contrary, Eastern Europe has experienced strong surface temperature increases in JA, particularly towards Ukraine and Russia. These tendencies are even stronger than the Iberian-Western Mediterranean MJ values.

From these results, it is evident that the remarkable temperature tendencies observed at Palma airport are not a local singularity but a regionally coherent feature. The maximum warming tendency in MJ is a striking fact, not exclusive of Palma or the Balearics, but extended to the whole Western Mediterranean region, including Iberia, France, and North-west Africa.

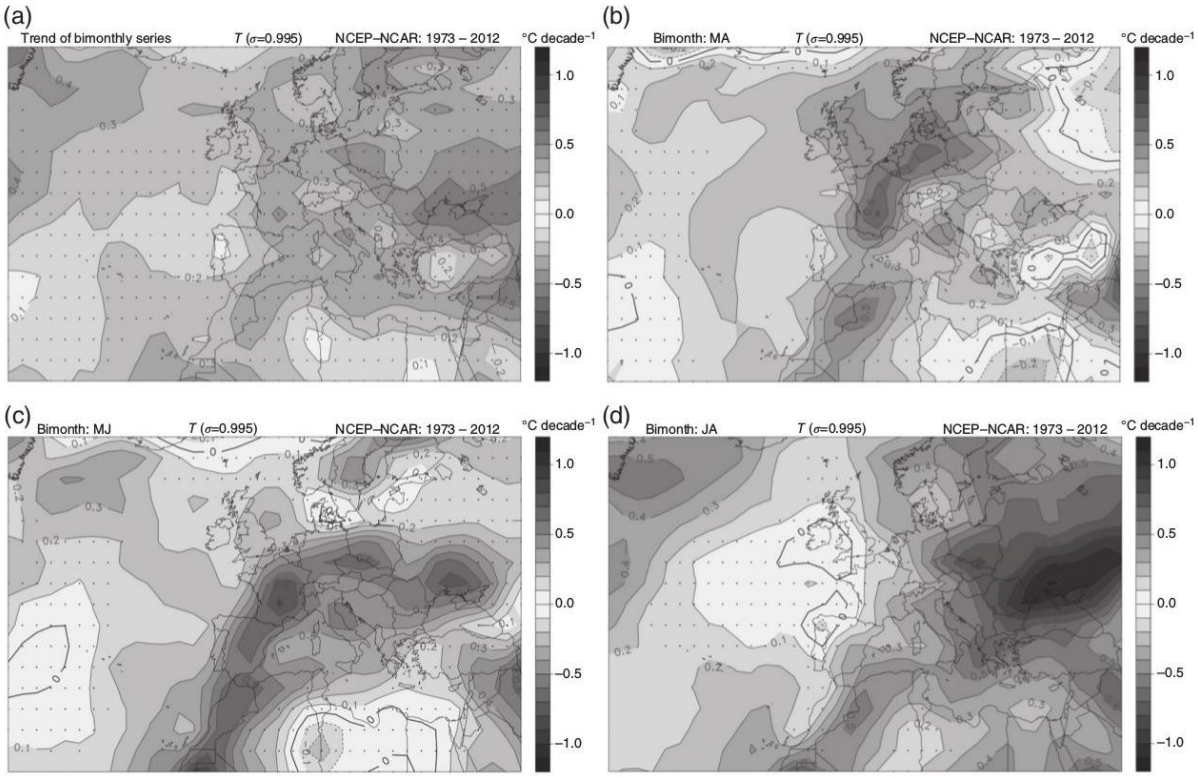

Figure 7: Analysis level σ = 0.995 temperature tendencies, °C decade−1, 1973–2012, for the whole year (a), MA (b), MJ (c) and JA (d). Negative tendencies are indicated with dashed contours. Dots indicate tendencies not significant at the 0.95 significance level.

4. Local Near-surface Temperature vs. 500 hPa Geopotential Height

According to the hypsometric equation, a relatively high correlation, and similar time tendencies between local near-surface temperatures and 500-GH values should be expected. Jansa (2012) already identify high correlations for the MJ series. However, purely dynamical factors can distort the correspondence between both variables, particularly in seasons with a high dynamical activity. For instance, upper-level potential vorticity anomalies produce divergence ahead, with upward motions and geopotential falls below (i.e. 500 hPa and below). This purely dynamic factor is independent of mid and low-level temperatures, and is very common under mid-latitude climatic regime with important cyclogenetic activity. When this dynamical mechanism becomes important, the correlation between 500-GH and surface temperature decreases.

In order to explore 500-GH tendencies and their correlation with the near-surface temperature throughout the year, monthly and bi-monthly values have been obtained taking the 2-m temperature average at the Palma airport and the 500-GH local average, with the NCEP_NCAR reanalysis being used for the latter (Table 2).

Table 2. Monthly and bi-monthly 1973-2012 tendencies for local temperature tendencies at Palma airport (TMP TND, ºC/10yrs) and for 500 hPa geopotential heights at the same point (500-GH TND, m/10yrs) and cross correlation between TMP and 500-GH (R). *(Statistically significant values at a confidence level of 95% are indicated in **bold** types).*

	TMP TND	500-GH TND	R		TMP TND	500-GH TND	R
Jan	0.11	0.4	-0.17	JF	0.06	3.7	0.30
Feb	0.01	6.9	**0.64**	MA	**0.58**	**11.9**	**0.63**
Mar	**0.40**	12.5	**0.57**	MJ	**0.72**	**12.2**	**0.84**
Apr	**0.78**	**11.4**	**0.51**	JA	**0.55**	**6.5**	**0.69**
May	**0.76**	**13.7**	**0.79**	SO	**0.45**	2.6	**0.66**
Jun	**0.70**	**10.7**	**0.76**	ND	0.22	-5.1	**0.34**
Jul	**0.56**	5.2	**0.63**	Year	**0.43**	**5.3**	**0.77**
Aug	**0.55**	**7.9**	**0.74**				
Sep	0.29	-3.7	**0.62**				
Oct	**0.60**	9.0	**0.64**				
Nov	0.40	-7.1	**0.42**				
Dec	0.05	-3.2	-0.14				

500-GH tendencies are weak, even negative, and statistically insignificant in winter or in late autumn or September, in line with the relatively low 2 m temperature tendencies. Note that the 500-GH tendency for MA is very high, but lower than for MJ. Additionally, spring 500-GH trends (both, MA and MJ) almost double those of pure summer months (JA). If the difference in tendency (about 6 m per decade) was sustained, the spring-summer 500-GH climatological difference would be cut in half in less than a century. Therefore, summer tends to extend towards spring when 500-GH is used as a season change indicator.

With regard to the temperature and 500-GH correlations, all monthly and bimonthly values are positive, large and statistically significant, except in winter. Correlations are not significant in December, January and JF, even coming in negative in December and January. Nevertheless, the largest correlations are obtained for May and June (consistent with the MJ bi-monthly results) and August. The R-value for MA is clearly lower than for MJ. Correlation coefficients are also only high and statistically significant for the warm half of the year (MJ, JA, SO), when two sub-periods (1973-1992 and 1993-2012) are considered. In addition, for MJ, JA and SO, the correlation coefficients are larger for the 1993-2012 than for 1973-1992, increasing from 0.79 to 0.84, 0.64 to 0.75 and 0.64 to 0.82, respectively.

Behaviour in MJ, as well as the higher correlation coefficient in the warm period (MJ, JA, SO) between sub-periods, supports the idea of a northward expansion of the tropical warm air dome (associated with high 500-GH values) during late spring, consistent with the idea of an earlier establishment of the Mediterranean summer conditions. But the equally strong secular increase of 500-GH in MA, without a parallel correspondence in the near-surface temperature tendency and with a weaker correlation of both variables, suggests that a substantial fraction of the MA 500-GH increase can be associated with the decrease in the cyclonic activity over the Mediterranean, a fact clearly detected in Guijarro et al. (2006). Note that the frequency of moderate or intense cyclones in the Western Mediterranean is relatively high from November to April and declines from May to October (Guijarro et al., 2006; Homar et al., 2007). The combination between increasing low-level temperatures and a still relatively high frequency of moderate and intense cyclones produces the spring minimum for sea level pressure that is observed in Palma in March and, particularly, in April (Fig. 4).

As the MJ period has the highest near-surface long term warming in Palma and largest 500-GH long-term local increase (with the highest correlation too), we examined 500 hPa regional patterns associated with thermal extreme MJ periods. The time series of near-surface temperature and 500-GH reveals that 1977 (2009) was one of the coldest (warmest) years in the period (Fig. 8). The 500 hPa mean fields for these two years show a very short-wave trough (in very cold MJ) or ridge (in very warm MJ) rather than a simple and general latitudinal shifting (southwards or northwards, respectively) of the 500-GH contour values, although some degree of shifting certainly exists.

5. Regional Patterns of 500 hPa Geopotential Tendencies

Although specific instances, the examples shown in Fig. 8 suggest that the intense warming observed near-surface, in the Iberian-Western-Mediterranean area, particularly in MJ, would be more related to a confined northwards expansion of a high 500-GH ridge-type feature (associated with the warm tropical air dome) than to the general shifting towards Europe of high 500-GH values. To verify this hypothesis, regional maps of 500-GH tendencies for bi-monthly periods have been obtained from the NCEP_NCAR reanalysis (Fig. 9).

As for the near-surface temperatures (Fig. 7), the 500-GH annual tendencies are not statistically significant (at 95% confidence level); neither are the 500-GH tendencies for JF, SO and ND in the Iberian-Western-Mediterranean zone (not shown). Only MA, MJ and JA show statistically significant 500-GH tendencies in that region.

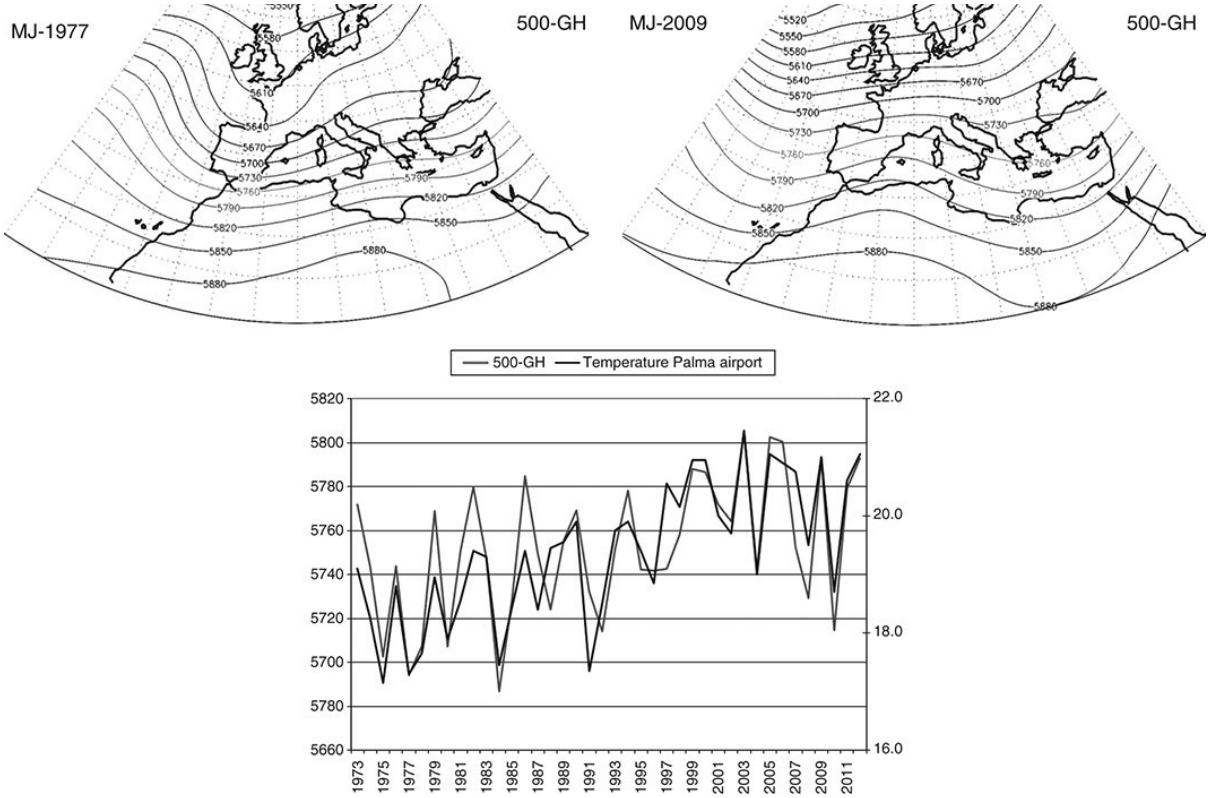

Figure 8: Simultaneous time series (1973–2012) of MJ average of near-surface temperature at Palma airport (homogenized series) and 500-GH above (c). Two extreme MJ periods are indicated with a circle in the time series (a very warm one, 2009, and very cold one, 1977). The corresponding 500 hPa geopotential patterns can be seen above, average 500-GH for MJ-1977 (a) and for MJ-2009 (b). (Raw Palma temperature data are from AEMET; 500-GH data and maps, from NCEP_NCAR reanalysis).

With regard to MJ and to the region of interest, an extensive 500-GH positive trend area covers the Iberian-West-Mediterranean zone, with a maximum (up to 16 gpm/decade) within France roughly coincident with the temperature tendency maximum (0.8ºC/decade) also found there (see Fig. 7 and section 3). In other words, the strong annual warming maximum of MJ over the Iberian-Western-Mediterranean area appears to be associated with the expansion of the subtropical upper air high pressures, in the form of a localised ridge reinforced towards the north. Note, as additional detail, that there is no relative minimum in the 500-GH increasing trend over the Western-Mediterranean maritime zone, as obtained for the low-level temperature in the reanalysis (Fig. 7) (but not with Balearic observations): the Western-Mediterranean maritime zone is fully affected by the pushing of subtropical upper air high pressure, even though the 500-GH maximum increase is not found there.

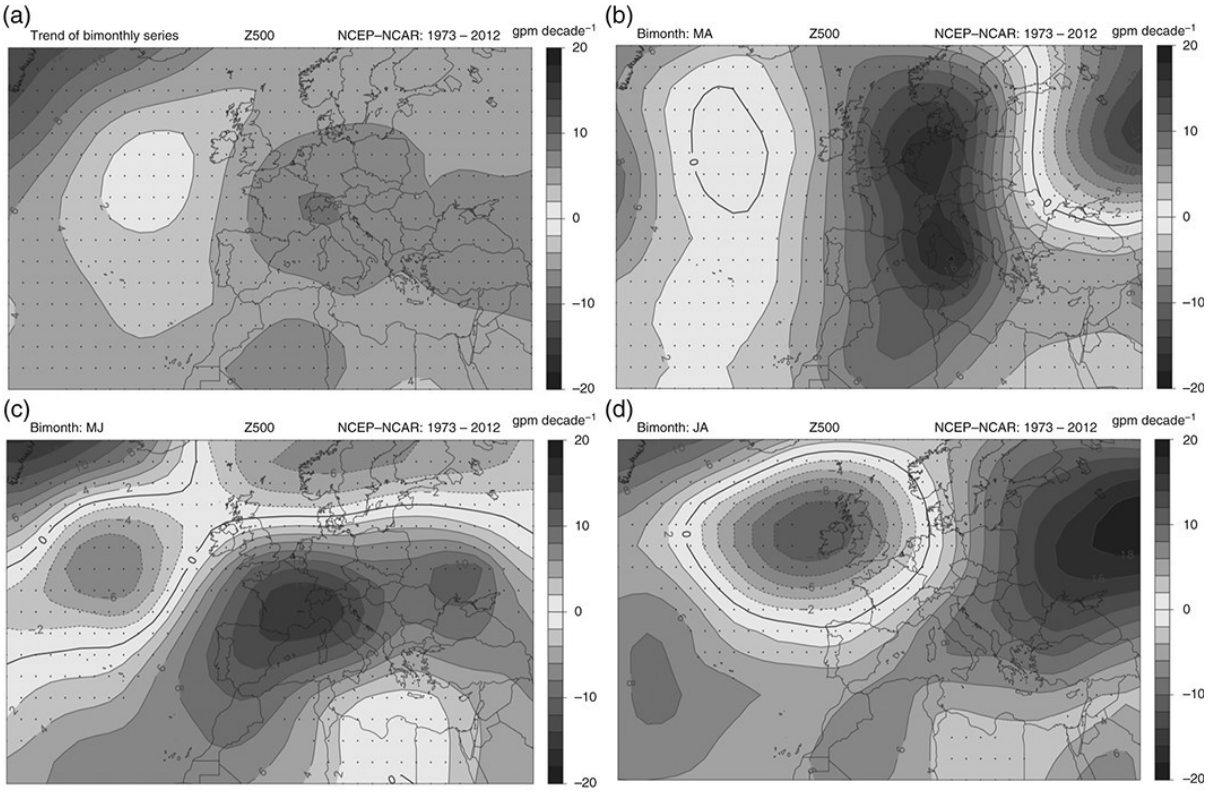

Figure 9: The 500 hPa geopotential height tendencies during 1973–2012, in gpm decade−1, for the whole year (a), MA (b), MJ (c) and JA (d). Negative tendencies are indicated with dashed contours. Note that the tendencies at grid points marked with a dot are not statistically significant at 95% level. (Source of raw data: NCEP_NCAR reanalysis).

The 500-GH tendency maxima in MA, which are even larger than the MJ maximum, are located in Northern-Europe (inland Germany) and in the Genoa-Tyrrhenian Sea, although the overlap with the near-surface maximum warming is not as good as in MJ. Note that the Genoa-Tyrrhenian maritime zone, which is an area of accentuated cyclonic activity in spring, does not exhibit any signal of maximum near-surface warming in MA; the closest warming maximum (around 0.6ºC/decade, more moderate than the MJ maximum) is located over inland France, collocated with the MJ main maximum. These results reinforce the idea from the section above, in the sense that a substantial part of the 500-GH increase in MA is linked to a decrease in the frequency of the cyclonic disturbances over the Mediterranean (Guijarro et al., 2006), rather than the expansion of the tropical warm air dome.

With regard to JA, a very strong positive 500-GH tendency maximum is identified towards Ukraine and Russia (with values exceeding 18 gpm/decade), in good spatial correspondence with the equally and very intense near-surface maximum warming (Fig. 7). In the Iberian-Western-Mediterranean zone, both near-surface warming and 500-GH increase for JA are clearly more moderate than in MJ.

6. Detection, Trends and Relevance of the Main May/June 500 hPa Geopotential Variability Patterns

The 500-GH average May/June values over a relatively large area around the Western Mediterranean (Fig. 9), and for 1973-2012 period have been analysed by means of principal components analysis in order to extract the main patterns of variability. Ten Varimax rotated principal components, explaining 83% of the sample variance, have been retained. The three patterns that explain the highest percentage of the total variance have been properly scaled to express the local correlation coefficients between the corresponding PC and the full original MJ 500-GH series (Fig. 10).

The patterns that explain most of the MJ 500-GH variability are not necessarily the most relevant patterns to account for the possible tendencies in the MJ 500-GH structure. Each 500-GH structure for every MJ of the series can be considered as almost entirely defined by the corresponding linear combination of scores over the retained PCs. Changes in the whole 500-GH structure during the period 1973-2012 would be the consequence of trends in the scores time series for, at least, some of the rotated PCs. Indeed, only those scores exhibiting significant trends would deserve special attention. We have computed the score trends for the main ten rotated PCs. The corresponding trend lies above 0.1 per decade only for two of these: the rotated PC1 and PC8. They are the constituents responsible for most of the decadal change in the whole MJ 500-GH field (Fig. 10 and Table 3). The substantial trends in the rot PC1 and rot PC8 suggest, respectively, important increases of MJ 500-GH in the Iberian-West-Mediterranean area and to the north-west of the Black Sea in relatively good alignment with the magnitude and location of the maximum increases directly inferred from the MJ 500-GH time series (Section 5 and Fig. 9).

The direct link between the identified patterns of variability of the MJ 500-GH field and the local temperature at Palma (TPal), or its temporal trend, has been explored firstly through deriving a multi-linear-regression (MLR) model for the temperature at Palma Airport (TPal), as a function of the pattern scores, and secondly, by processing the previous score trends through this model (Table 3).

The model we are looking for is of the type:

$$\mathrm{MLR} = b0 + \sum_{1}^{10} \mathrm{bi} \cdot \mathrm{PCi}$$

where *PCi* are the *i* scores and *bi* the corresponding linear coefficients.

The MLR obtained in this way is very robust in describing the variability of TPal. Fig. 11 shows the very good alignment between MLR-modelled and TPal-observed local 2 m temperatures. The correlation coefficient between both series is as high as 0.919, and the root mean square error is only 0.46ºC. The standard deviation of the

temperature series in Palma, MJ 1973-2012 is 1.18°C, much higher than the root mean square error of the adjustment. This means that the average MJ local near-surface temperature at Palma airport is very well described by large scale mid-tropospheric structures. As observed in Table 3, PC1, PC2, PC6 and PC8 are the most influential components on temperature variability in Palma.

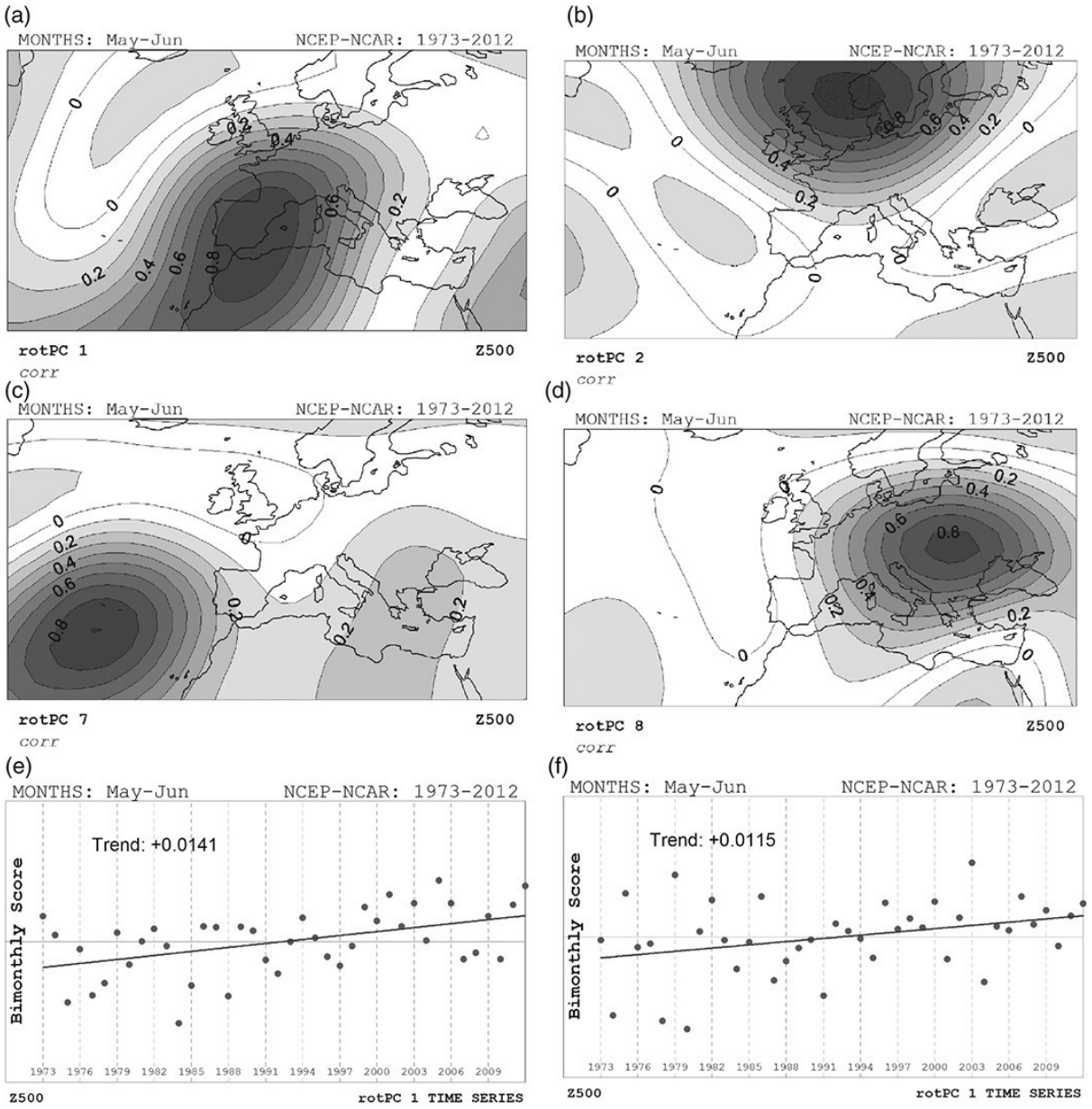

Figure 10: Correlation coefficients defining the three main rotated PC of the MJ average 500-GH fields, during the 1973–2010 period, regarding the variance explained (rot PC1, PC2 and PC7, (a–c) maps, respectively) and the two rotated PCs with the largest trend along 1973–2012 (rot PC1 and PC8, (a) and (d) maps, respectively). In (e) and (f), time series of scores associated to rot PC1 and PC8 are shown.

Table 3. Multi-linear-regression (MLR) model for the local near-surface temperature at Palma (TPal), given by the combination of rotated PC scores (bi = coefficients in the MLR model, ºC), tendencies of the rot PC scores (PCT, per decade) and contribution of the PC trends to the TPal tendency (CTPT = bi x PCT, ºC/decade)

TPal		PC1	PC2	PC3	PC4	PC5	PC6	PC7	PC8	PC9	PC10
bi	19.38	**2.54**	**1.20**	0.70	0.66	0.16	**1.08**	0.05	**1.38**	0.88	0.39
PCT		**0.14**	-0.03	0.09	0.05	0.04	-0.04	0.05	**0.12**	0.07	-0.05
CTPT	**0.58**	**0.36**	-0.03	0.06	0.03	0.01	-0.05	0.00	**0.16**	0.06	-0.02

The first bi (b0) is the independent term on the MLR model.

The total contribution of the ten PC trends to the local temperature tendency at Palma is 0.58ºC/decade, which is the sum of all the 10 CTPT terms.

The contribution of the PC trends to the TPal tendency can also be explored through the MLR model by means of combining the MLR equation coefficients with the PC score trends. Despite PC1, PC2, PC6 and PC8 being identified as the most relevant components for TPal value, not all of them significantly influence the TPal tendency (Table 3). In particular, since PC2 and PC6 have no significant trend, they become irrelevant for explaining the local temperature increase in Palma.

Leaving aside the residual variance associated with the rest of non-retained PCs, it is obvious that many local and sub-regional scale factors can also affect the variability and tendency of TPal. For this reason, it is a remarkable that with ten principal components of the large-scale 500-GH field, we can explain most of the increase, namely 0.58ºC/decade, which is 81% of the total observed trend of 0.72ºC/decade. Note, in this sense, the primary influence on TPal of the trend of PC1) alone, which explains half of the total observed TPal trend. The positive trend of PC1 can be described as a robust decadal increase of 500-GH in a large ridge-shaped area, covering Iberia, the Western Mediterranean, France and Northwest Africa (Fig. 10). The contribution of the PC8 trend is less, but nevertheless important, and means an anticyclonic reinforcement across Eastern Europe, thus consistent with an enhancement of the southerly advection over the Western Mediterranean area.

7. Discussion and Conclusions

The most important contribution of our study is the correlation between the temporal variations in the low-level temperature and the upper-level geopotential height. The increase in this correlation during spring denotes the onset of the summer while the positive trend of both magnitudes we have found along our study period indicates a stretching of the summer season towards the spring.

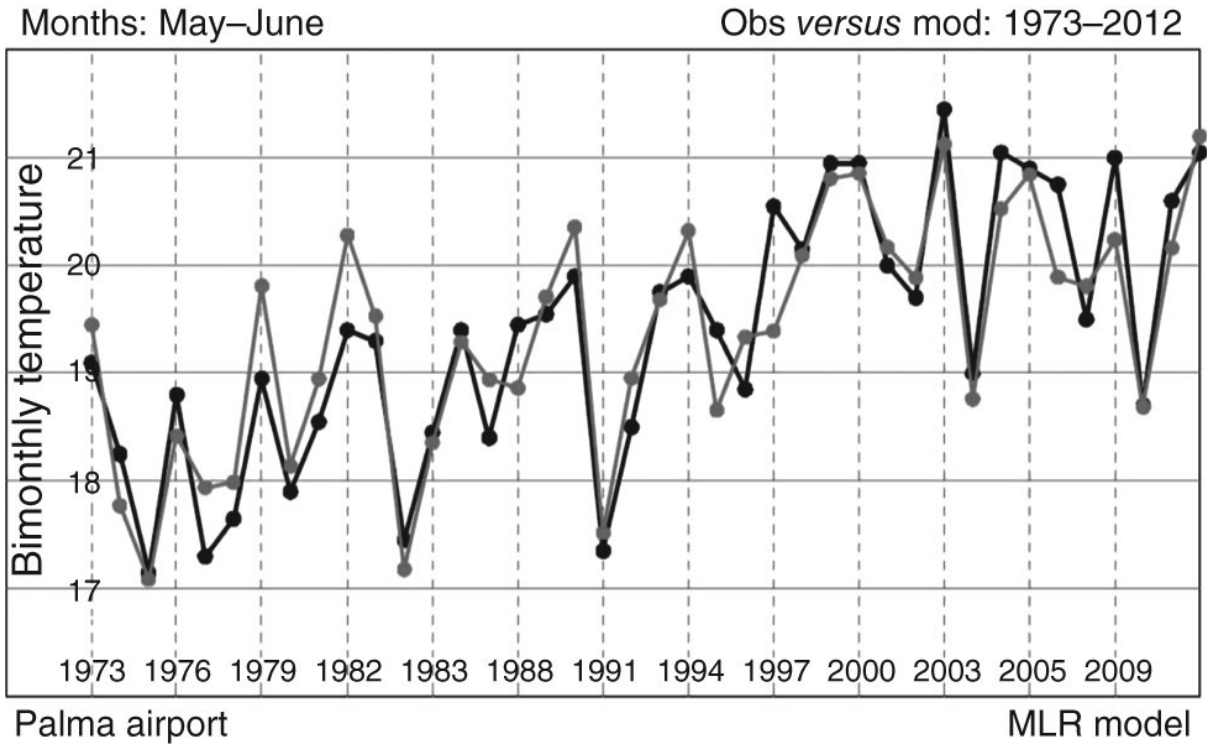

Figure 11: Observed (black line) versus modelled (grey line) local 2 m temperature at Palma airport, using a multi-lineal-regression based on the main ten rotated PC obtained from the MJ 500-GH field in a large domain around Palma.

In the context of climate change, Yin (2005) introduced the idea of a poleward contraction of the mid-latitude cyclone tracks. This idea would imply a latitudinal widening of the Hadley Cells. Hu and Fu (2007), Lu et al. (2007) or Seidel and Randel (2007), among others, have been explicit in pointing out an expansion or widening of the Hadley circulations, using observational evidence or modelling results. Recent papers (such as Hu et al., 2011) have corroborated the former results, with more data and more elaborated procedures. IPCC (2013) and Birner et al. (2014) have updated and summarised the findings about the widening of the HCs. These authors used heterogeneous sources of data and different criteria or methodologies to define the HC bounding limits and thus their hypothesised expansion during the last decades. Zonal bands of minimum precipitation, maximum sea level pressure or maximum outgoing long wave radiation are some of the criteria used. Another method comprises computing the Stokes mass mean meridional streamfunction (Hartmann, 1994) from reanalysis, which is a very indicative procedure. However, when the mass streamfunction is evaluated through integration along the whole latitudinal circle, summer seasons show weak and confusing structures (Dimas and Wallace, 2003; Cook, 2005).

There are some ways to approach the seasonality problem when analysing the possible expansion or widening of the HC in depth. One possible method is the use of a dynamical definition of the HCs edges; Kang and Lu (2012), for instance, have

used the Held (2000) definition based on the presence of baroclinic instability. This kind of criterion enables identification of the polar edge of the HC in winter and summer, when it shifts poleward. The widening of the HC can also be established in this way in winter and summer separately.

The shifting of the subtropical jet and the characterisation of the subtropical anticyclones are alternative ways to identify seasonal changes in the tropical circulation, as well as any trend in the expansion of the HC (Fu and Lin, 2011; Li et al., 2012). In terms of subtropical anticyclones, Li et al. (2012) have stressed their summertime intensification, both in the recent historical period and in future projection. This intensification is identified at low levels (925 hPa), but only over oceanic areas.

In this paper we have explored the temporal changes for the start of summer and its relation to a possible expansion of the HC. The underlying concept is that the edge of the HC is occupied by deep and warm subtropical anticyclones. For the identification of these anticyclones in regions with complex terrain, as the Iberian West Mediterranean region in general and the Balearic area in particular, sea level pressure or low-level geopotential height are not useful indicators. In contrast, the 500-GH fields provide good information for this purpose, even though their magnitude is relatively uniform across the tropical and subtropical latitudes. Isolated subtropical or Mediterranean latitude 500-GH positive anomalies (i.e. high level subtropical isolated anticyclones) are difficult to be found in a climatological sense, but high 500-GH values can indirectly indicate the presence of a warm tropical dome, i.e. the presence of the HC edge.

Selection of a particular value of 500-GH as a quantitative indicator of the presence (or not) of the HC edge and, correspondingly, of the Mediterranean summer onset, duration or intensity, could be appropriate in some areas, but any particular chosen value would contain a certain degree of arbitrariness. In section two, the 5800 gpm value of 500-GH was identified as a possible summer onset indicator in the Balearic region. However, when dealing with the variability and temporal tendency of the HC, rather than with the average position of any isohypse, it is better to examine the changes of the 500-GH field itself. When looking at the 1981-2010 averages, the difference between MJ (late spring) and JA (full summer) is about 100 gpm over Palma; according to the 500-GH observed tendencies, this difference would fall to about 50 gpm in 40 years. The extension of summer climatic conditions into late spring in the Western Mediterranean area, manifested on the accentuated temperature trends of the MJ period, is explained, confirmed and interpreted through the expansion of the warm tropical dome of high 500-GH values. Note that an increase of 50 gpm in average 500-GH over 40 years can be viewed as a mean anticipation of the summer of about one month.

Our results are clearly consistent with a HC widening, although our reference is neither planetary nor annual, but limited to late spring and to the Western

Mediterranean region, including the surrounding territories. Mainly affecting a ridge-shaped area, the HC edge expansion is more important in the Iberian West Mediterranean region, including France and Northwest Africa (with a less pronounced maximum in Eastern Europe), rather than in farther-field areas, at least in MJ.

Results from previous studies indicate that for the planetary and annual context, the magnitude of the observed expansion of the Hadley Cells are found in the range of 1 to 4 latitude degrees in each hemisphere during nearly 40 years, depending on the indicators and methodology used (IPCC, 2013, and Birner, 2014 for a summary). When comparing tendencies and spatial gradients of 500-GH, our results indicate that in the Iberian West Mediterranean in late spring, the widening we obtain would be sited in the higher part of the cited range, with around 3 or 4 degrees of latitude over 40 years.

Acknowledgments

This work was partially supported by EXTREMO (CGL2014-52199-R) project, funded by the Spanish Ministry of the Economy and Competitiveness, with partial contribution from FEDER funds.

The performance and availability of the different datasets used in this work is due to institutions like AEMET (Spain), NCEP, NCAR or NOAA/ESRL (USA) and ECMWF. We wish to express our acknowledgment to all of them. Some of the data from AEMET have been taken online, from http://www.aemet.es/es/conocermas/publicaciones/detalles/guia_resumida_2010 (accessed in 2014). Some data from the NCEP_NCAR reanalyses were also taken also online, from the NOAA/ESRL Physical Sciences Division facilities (accessed in 2014).

We are grateful to Radan Huth, editor, to Baruch Ziv, referee, and to an anonymous referee for their useful comments and suggestions, which have clearly contributed to improve the quality and understanding of this paper.

References

Argüeso, D., J. M. Hidalgo-Muñoz, S. R. Gámiz-Fortis, M. J. Esteban-Parra, and Y. Castro-Díez, 2012: High-resolution projections of mean and extreme precipitation over Spain using the WRF model (2070–2099 versus 1970–1999), Journal of Geophysical Research, 117, D12108, doi:10.1029/2011JD017399.

Barry, R.G., and R.J. Chorley, 2010 [Ninth edition]: Atmosphere, weather and climate, Routledge, Taylor and Francis Group, London and New York, 516 pp.

Belda, M., E. Holtanová, T. Halenka and J. Kalvová, 2014: Climate classification revisited: from Köppen to Trewartha, Clim. Res., Vol. 59: 1–13, doi: 10.3354/cr01204Birner, T., S.M. Davis and D.J. Seidel, 2014: The changing width of Earth's tropical belt, Physics Today, 67(12), 38 (2014); doi: 10.1063/PT.3.2620, online: http://dx.doi.org/10.1063/PT.3.2620

Bladé I. and Castro Díez Y., 2010: Atmospheric trends in the Iberian Peninsula during the instrumental period in the context of natural variability. Report: Climate in Spain: Past, Present and Future (Editors: Pérez F. Fiz and Boscolo Roberta) pp. 25–41.

Blumler, M.A., 2005: Three Conflated Definitions of Mediterranean Climates, Middle States Geographer, 2005, 38: 52-60.

Cook, K.H., 2005: Hadley circulation dynamics: seasonality and the role of continents, in The Hadley Circulation: Present, Past and Future, Diaz, Henry F., Bradley, Raymond (Eds.), Springer series: Advances in Global Change Research, Vol. 21, published by Kluwer Academic Publishers, pp 61-83.

De Castro, M, Gallardo, C, Jylha, K, Tuomenvirta, H, 2007: The use of a climate-type classification for assessing climate change effects in Europe form an ensemble of nine regional climate models. Clim Change 81: 329−341.

Del Río, S., L. Herrero, C. Pinto-Gomes, A. Penas, 2011: Spatial analysis of mean temperature trends in Spain over the period 1961–2006, Global and Planetary Change, 78, 65–75.

Dimas, I.M., and J.M. Walace, 2003: On the Seasonality of the Hadley Cell, J. Atmos. Sci., 60, 1522-1526.

Fu, Q., and P. Lin, 2011: Poleward Shift of Subtropical Jets Inferred from Satellite-Observed Lower-Stratospheric Temperatures. J. Climate, 24, 5597-5603.

Gallardo, C., V. Gil, E. Hagel, C. Tejeda and M. de Castro, 2013: Assessment of climate change in Europe from an ensemble of regional climate models by the use of Koppen–Trewartha classification, Int. J. Climatol., 33, 2157–2166, DOI: 10.1002/joc.3580.

Gaussen, H., 1955 : Détermination des climats par la méthode des courbes ombrothermiques. Comptes Rendus Hebdomadaires Des Seances De L Academie Des Sciences 240.6: 642-643.

Guijarro, J.A., A. Jansa and J. Campins, 2006: Time variability of cyclonic circulation in the Mediterranean, Advances in Geosciences, 7, 45-49, SRef-ID: 1680-7359/adgeo/2006-7-45.

Guijarro, J. A., 2014: User's Guide to Climatol. 40 pp. http://www.climatol.eu/climatol-guide-pdf

Guijarro, J.A., 2013: Temperature trends, in Adverse weather in Spain, C. García-Legaz and F. Valero (Eds.), Madrid, AMV Ediciones, 297-306.

Hartmann, D.L., 1994 : Global Physical Climatology, Academic Press, San Diego, New York, Boston, London, Sydney, Tokyo and Toronto, 408 pp.

Held, I. M., 2000: The general circulation of the atmosphere. Proc. Geophysical Fluid Dynamics Program, Woods Hole, MA, Woods Hole Oceanographic Institute, 1–70. [Available online at http://gfdl.noaa.gov/cms-filesystem-action/user_files/ih/lectures/kwoods_hole.pdf.]

Homar, V, A. Jansa, J. Campins, A. Genoves, and C. Ramis, 2007: Towards a systematic climatology of sensitivities of Mediterranean high impact weather: a contribution based on intense cyclones, Nat. Hazards Earth Syst. Sci., 7, 445–454, www.nat-hazards-earth-syst-sci.net/7/445/2007/

Homar, V, C. Ramis, R. Romero and S. Alonso, 2010: Recent trends in temperature and precipitation over the Balearic Islands (Spain). Climatic Change, DOI 10.1007/s10584-009-9664-5.

Hoskins, B., 1996: On the Existence and Strength of the Summer Subtropical Anticyclones. Bernard Haurwitz Memorial Lecture, Bull. Amer. Meteor. Soc., 77, nº6, 1287-1292

Hu, Y. and Q. Fu, 2007: Observed poleward expansion of the Hadley circulation since 1979. Atmos. Chem. Phys., 7, 5229–5236.

Hu, Y., Zhou, C., and Liu, J., 2011: Observational Evidence for Poleward Expansion of the Hadley Circulation. Advances In Atmospheric Sciences, Vol. 28, No. 1, 2011, 33–44.IPCC, 2013: Climate Change 2013: The Physical Science Basis. Contribution of Working Group I to the Fifth Assessment Report of the Intergovernmental Panel on Climate Change [Stocker, T.F., D. Qin, G.-K. Plattner, M. Tignor, S.K. Allen, J. Boschung, A. Nauels, Y. Xia, V. Bex and P.M. Midgley (eds.)]. Cambridge University Press, Cambridge, United Kingdom and New York, NY, USA, 1535 pp, doi:10.1017/CBO9781107415324.

Jansa, A., 2012. Primavera i canvi climatic (Climatic change and spring; in Catalan). Territoris (Universitat de les Illes Balears). Num. 8, pp. 129-142, ISSN: 1139-2169.

Kalnay et al., 1996, The NCEP_NCAR 40-year reanalysis project, Bull. Amer. Meteor. Soc., 77, 437-470.

Kang, S. and J. Lu, 2012: Expansion of the Hadley Cell under Global Warming: Winter versus Summer, J. Clim., 25, 8387-8393.

Köppen, W.,1900: Versuch einer Klassifikation der Klimate, vorzugsweise nach ihren Beziehungen zur Pflanzenwelt. Geographische Zeitschrift6, 657–679.

Köppen, W., Geiger, R., 1930: Handbuchder Klimatologie. Gebrueder Borntraeger, Berlin.

Li, W., L. Li, M. Ting and Y. Liu, 2012: Intensification of Northern Hemisphere subtropical highs in a warming climate, Nature Geoscience, DOI: 10.1038/NGEO1590.

Lionello, P., F. Abrantes, L. Congedi, F. Dulac, M. Garcic, D. Gomis, C. Goodess, H. Hoff, H. Kutiel, J. Luterbacher, S. Planton, M. Reale, K. Schröder, M.V. Struglia, A. Toreti, M. Simplis, U. Ulbrich and E. Xoplaki, 2012: Introduction: Mediterranean Climate – Background Information, in P. Lionello, ed., The Climate of the Mediterranean Region, from the Past to the Future. Elsevier, Amsterdam. 502 pp.

Lu, J., G. A. Vecchi and T.Reichler, 2007: Expansion of the Hadley cell under global warming. Geophysical Research Letters, Vol. 34, L06805, doi:10.1029/2006GL028443.

Peel, M.C., Finlayson, B.L., McMahon, T.A., 2007: Updated world map of the Köppen-Geiger climate classification. Hydrol Earth Syst Sci 11: 1633−1644Rodwell, M.J., and B.J. Hoskins, 1996: Monsoons and the dynamics of deserts, Q. J. R. Meteorol. Soc., 122, 1385-1404.

Seidel, D. J., and W. J. Randel, 2007: Recent widening of the tropical belt: Evidence from tropopause observations. J. Geophys. Res., 112, D20113, doi: 10.1029/2007JD0 08861.

Trewartha, G.T., Horn, L.H. (1980) Introduction to climate, 5th edn. McGraw Hill, New York, NY.

Trigo, R., E. Xoplaki, E. Zorita, J. Luterbacher, S.O. Krichak, P. Alpert, J. Jacobeit, J. Saenz, J. Fernandez, F. Gonzalez-Rouco, R. Garcia-Herrera, X. Rodo, M. Brunetti, T. Nanni, M. Maugeri, M. Türkes, L. Gimeno, P. Ribera, M. Brunet, I.F. Trigo, M. Crepon and A. Mariotti, 2006: Chap. 3: Relations between Variability in the Mediterranean Region and Mid-Latitude Variability, in Mediterranean Climate Variability (edited by P. Lionello, P. Malanotte-Rizzoli and R. Boscolo), Elsevier, Amsterdam, pp 179-226.

Yin, J.H., 2005: A consistent poleward shift of the storm tracks in simulations of 21st century climate. Geophysical Research Letters, Vol. 32, L18701, Doi:10.1029/2005gl023684, 2005.

Ziv, B., H. Saaroni and P. Alpert, 2004: The Factors Governing the Summer Regime of the Eastern Mediterranean, Int. J. Climatol., 24, 1859–1871.

Ziv, B., H. Saaroni, R. Pargament, T. Harpaz and P. Alpert, 2013, Trends in rainfall regime over Israel, 1975-2010, and their relationship to large-scale variability, Regional Environmental Change, 14:1751–1764.